Supplement of Weather Clim. Dynam., 7, 873–893, 2026
https://doi.org/10.5194/wcd-7-873-2026-supplement

Supplement of

Identifying controls of extratropical cyclone intensity at genesis time and during intensification in the North Atlantic and Europe

Joona Cornér et al.

Correspondence to: Joona Cornér (joona.corner@helsinki.fi)

S1 Intensity measure distributions

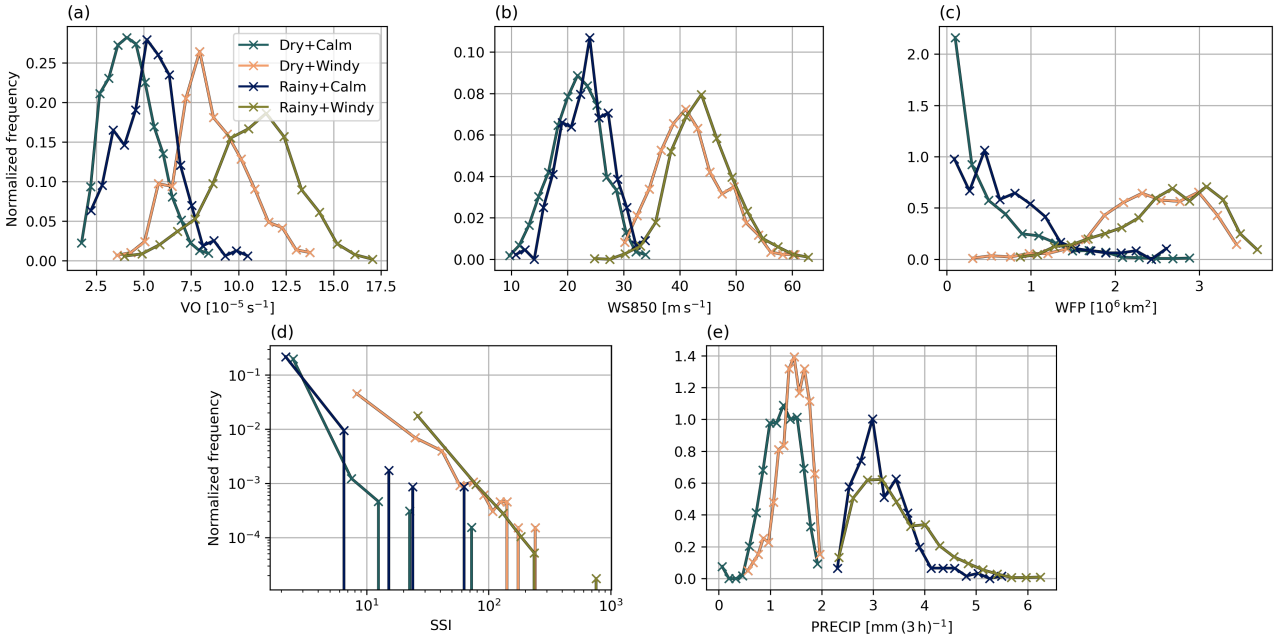

Figure S1. Distributions of the five intensity measures in the four intensity groups (shown in the legend in panel **(a)**). All measures are analysed at the time of maximum VO along each track except for PRECIP which is 12 h before the time of maximum VO.

S2 Full intensity group sensitivity fields

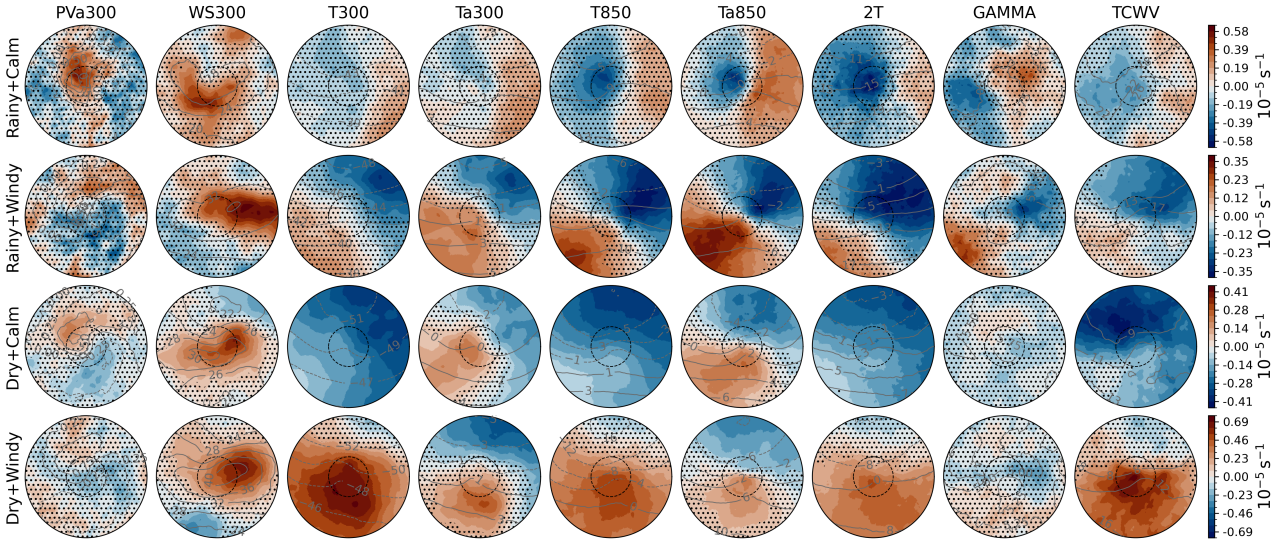

Figure S2. Sensitivity signals of VO (shading) for each intensity group and the composite field of precursors at genesis (contours). Intensity groups stay constant along rows and precursors stay constant along columns. There is one colourbar per intensity group, i.e. per row. The hatched areas indicate statistically nonsignificant values and the dashed black circle denotes a radius of 6° geodesic. The radius of the whole circle is 18° geodesic. Units of precursors are PVU ($10^{-6}\,\mathrm{K\,m^2\,kg^{-1}\,s^{-1}}$) for PVa300, $\mathrm{m\,s^{-1}}$ for WS300, °C for T300, Ta300, T850, Ta850, and 2T, $^\circ\mathrm{C\,km^{-1}}$ for GAMMA, and $\mathrm{kg\,m^{-2}}$ for TCWV.

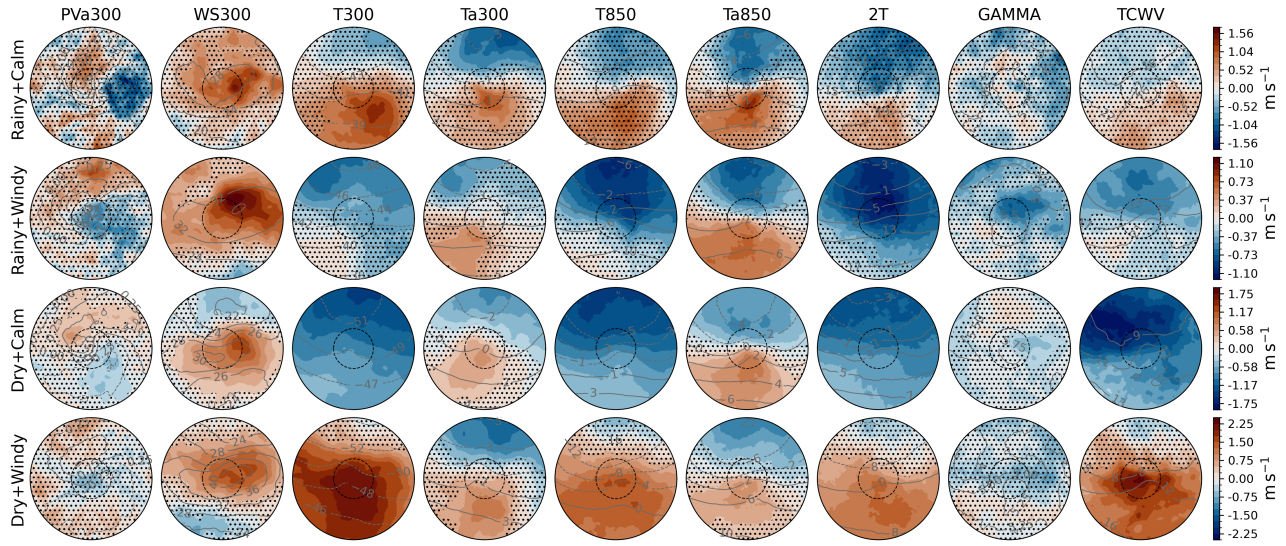

Figure S3. As in Fig. S2 for WS850.

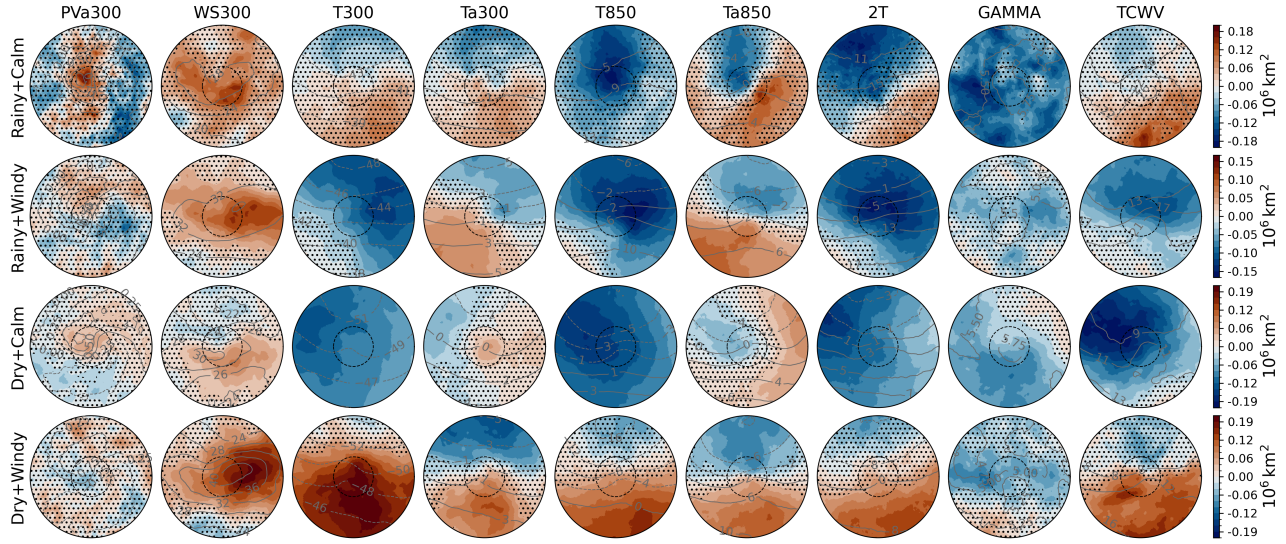

Figure S4. As in Fig. S2 for WFP.

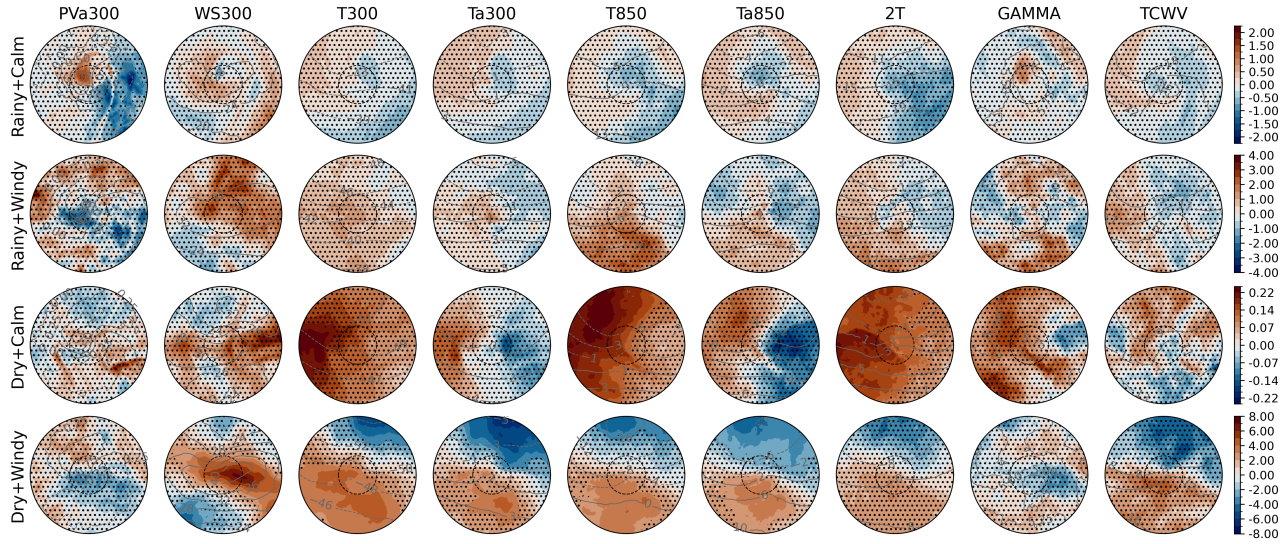

Figure S5. As in Fig. S2 for SSI.

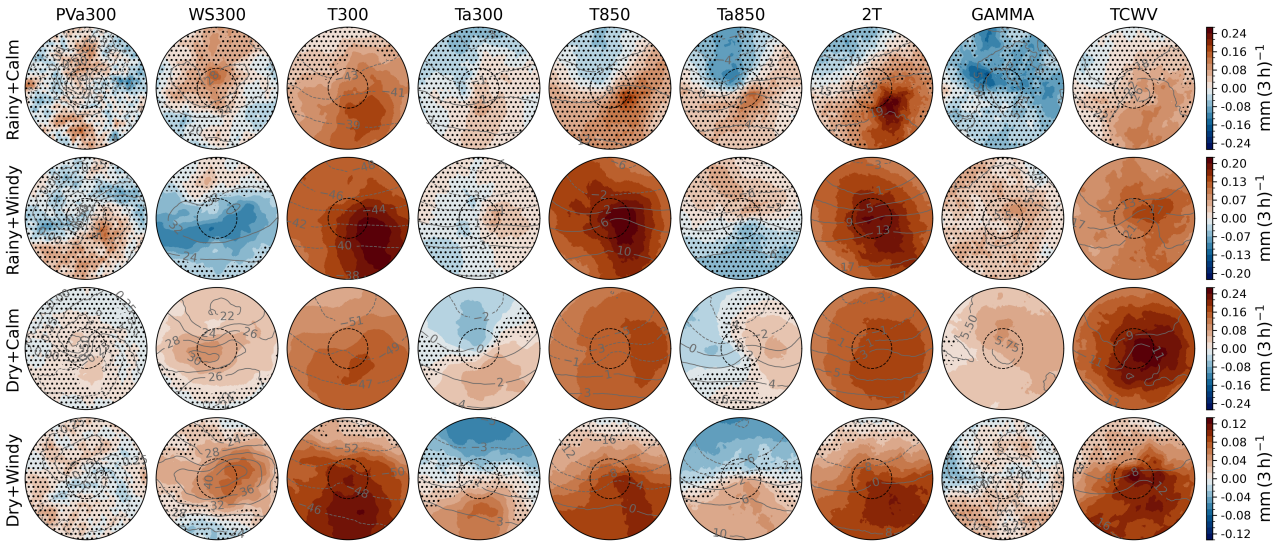

Figure S6. As in Fig. S2 for PRECIP.

S3 Precursor climatologies and their effect on sensitivity patterns

To further understand and interpret the sensitivity signals for all extratropical cyclones (ETCs) and in the four intensity groups, we can consider where geographically ETC genesis in the groups occurs. As discussed in Sect. 2.5, Fig. 2 of the manuscript shows where ETCs with certain intensity characteristics (e.g. Windy or Rainy) preferentially occur and Fig. S7 from where they originate. This information can be combined with climatological distributions of the precursors to understand their potential influence on the sensitivity fields. Here, climatology refers to mean values of the extended winter season (October–March, ONDJFM) between the years 1979 and 2022. Climatological distributions of precursors discussed in the following text are shown in Figs. S8–S12.

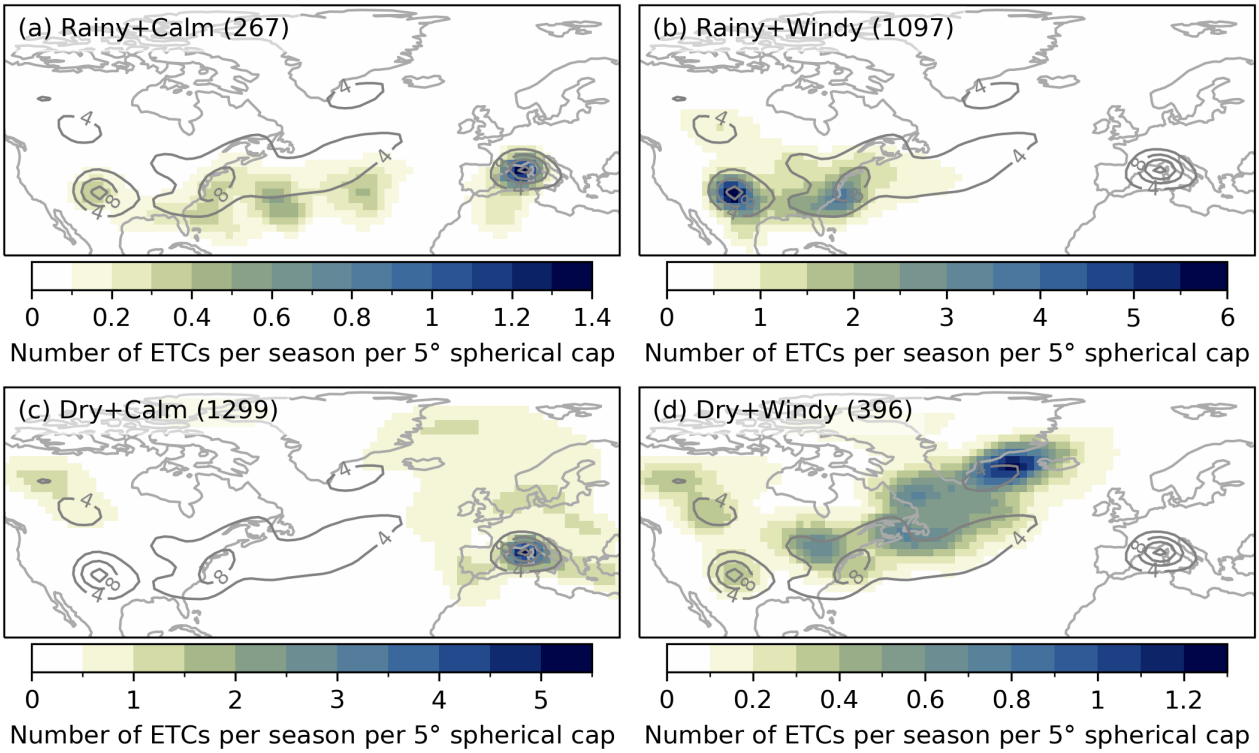

Figure S7. Genesis densities of the four intensity groups. The value indicates the number of ETCs originating from an area within a spherical cap with a radius of 5° geodesic per season (six months). The contours show the genesis density distribution of the full dataset (7361 ETCs) in the same unit. Total number of ETC tracks in each group is shown in the parentheses. Note the different values in the colourbars.

For example, from the track density distributions in Fig. 2 in the manuscript it is evident that Windy ETCs occur mostly along the main storm track. This is well inline with the results of the ensemble sensitivity analysis for the full dataset which indicate that large wind intensity is associated with a strong jet stream. The pattern with the largest positive WS300 sensitivity values to wind intensity occurring downstream of the ETC centre can be interpreted as ETCs having their genesis more in the right hand entrance of a jet streak. However, it is also possible to understand the pattern from a climatological perspective. ETCs which originate from the beginning of the storm track, i.e. mostly Windy ETCs, develop stronger winds (Figs. S7 and S8). The strong positive sensitivity signals from T300 support this, as the start of the storm track is climatologically warmer than the end due to the southwest–northeast tilt (Fig. S9). The right hand entrance of a jet streak is also warmer than the core based on the thermal wind law, and the jet is more often than not oriented zonally based on the climatology. At lower

levels in which the climatological temperature distribution tilts more towards northeast with the storm track (Fig. S10), the overall temperature distribution is less important, and it is the strength of the thermal gradient (Ta850) – a more transient feature – which has more control on the wind intensity.

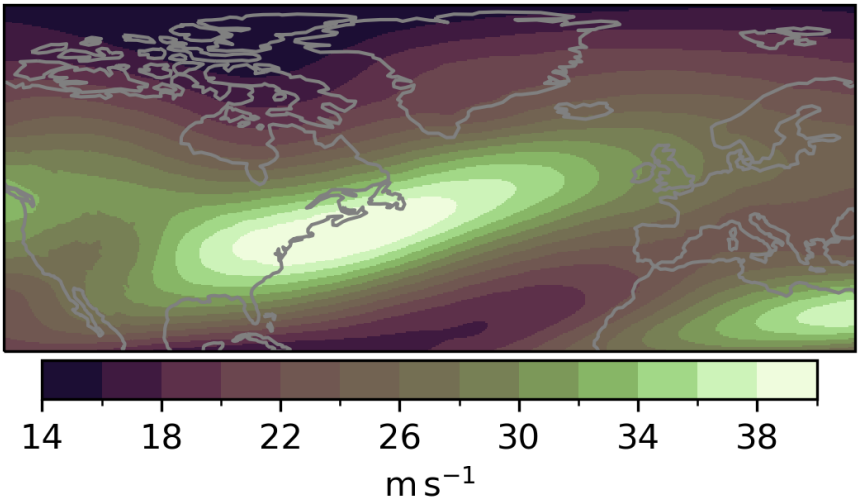

Figure S8. Climatological mean values of WS300 during ONDJFM 1979–2022.

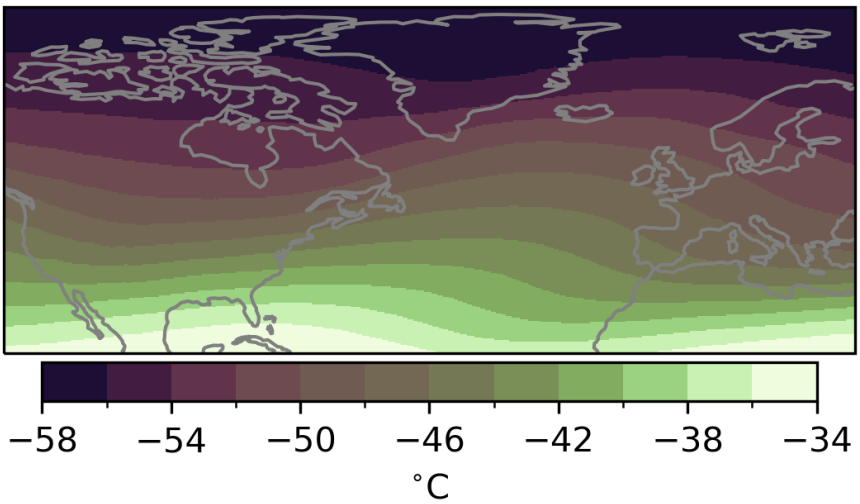

Figure S9. Climatological mean values of T300 during ONDJFM 1979–2022.

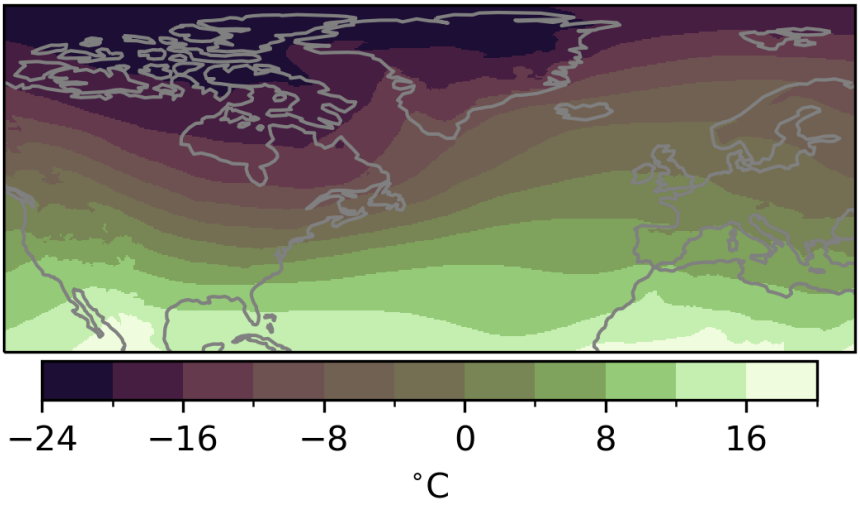

Figure S10. Climatological mean values of T850 during ONDJFM 1979–2022.

For PRECIP the correspondence of the ensemble sensitivity analysis (ESA) results with the track and genesis density distributions and the precursor climatologies is straightforward. Compared to their Dry counterparts, Rainy ETCs occur more in the southern parts of the domain which climatologically have more moisture available (Fig. S11) and higher temperatures. This is exactly what we see in the ESA for the full ETC dataset as well.

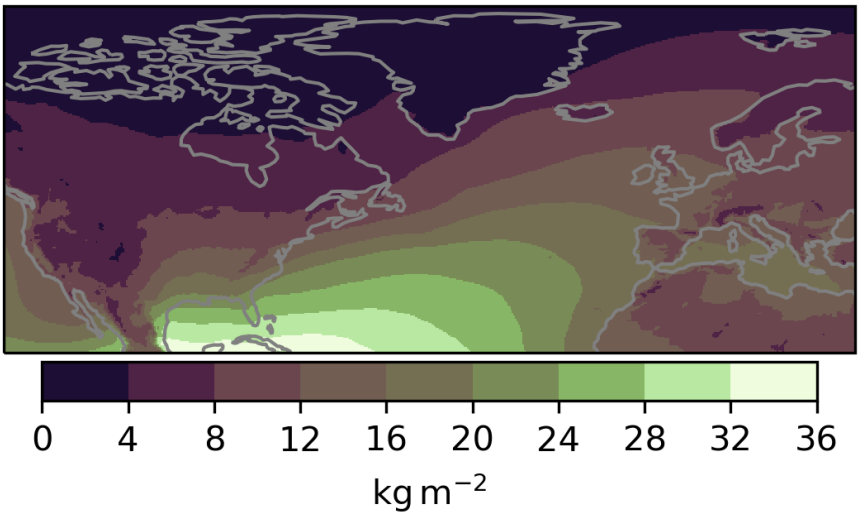

Figure S11. Climatological mean values of TCWV during ONDJFM 1979–2022.

As for the sensitivity signals (Fig. 5 in the manuscript) and patterns (Figs. S2–S6) in the four intensity groups discussed in Sect. 3.2 of the manuscript, many of the sensitivity signals and patterns in the intensity groups do not have evident explanations based on theoretical expectations. However, as in the full dataset, we can attempt to understand some of them via climatological conditions.

Climatological conditions affecting the genesis environment could explain, for example, why wind intensity in group Dry+Windy is so sensitive to T300. Group Dry+Windy has plenty of ETCs along the full extent of the main storm track (Fig. 2d in the manuscript) and especially the most varied genesis locations (Fig. S7d). ETCs closer to the start of the storm track are on average more intense than ones closer to the end (Dacre and Gray, 2013; Binder and Wernli, 2025; Cornér et al., 2025). Like the average intensity, the climatological T300 field has

decreasing values along the storm track (Fig. S9), hence the strong sensitivity to T300 in group Dry+Windy. Similarly, wind intensity in group Dry+Calm is negatively sensitive to temperature and TCWV. This indicates that ETCs whose genesis is more northerly – specifically in this group outside the Mediterranean – have stronger winds (Fig. S7c). The reason why PRECIP in group Dry+Calm is especially sensitive to TCWV is the same, with the added effect of limited moisture availability in the northern parts of the domain (Pfahl and Sprenger, 2016). In these areas relatively small changes in TCWV would thus lead to much more precipitation.

It should be noted that while climatological conditions likely affect the genesis and development of ETCs to some extent, and ETCs contribute to the climatological mean state, for transient phenomena like ETCs, the genesis states deviate from the climatology from case to case by definition. This is evident in our results since the variation in a precursor field is as large as differences between the precursor composite means of the intensity groups (not shown). In an individual intensity group the genesis conditions are more homogenous than in the full dataset, which means that this caveat becomes less relevant. However, the track and genesis density distributions (Figs. 2 and S7) have overlap between the groups and therefore do not represent unique climatological conditions in the first place.

An example of this – a precursor genesis field not matching the climatological state – is GAMMA in the Windy intensity groups. Their genesis composites show relatively small GAMMA values (Fig. S12), which agrees with the results of the ESA in the full dataset. However, the Windy ETCs have genesis hot spots in the Rocky Mountains (Rainy+Windy) and between Greenland and Iceland (Dry+Windy, Fig. S7), areas with climatologically large GAMMA values (Fig. S12). In fact, the area with the smallest climatological GAMMA values in the domain, the Labrador Peninsula (Fig. S12 and Mbengue et al., 2019), has almost no occurrences of cyclogenesis (Fig. S7). Therefore, especially since the negative GAMMA sensitivities do not match theoretical expectations (as discussed above), their interpretation is autocorrelation with opposing perturbations in the temperature precursors at 300 hPa and 850 hPa.

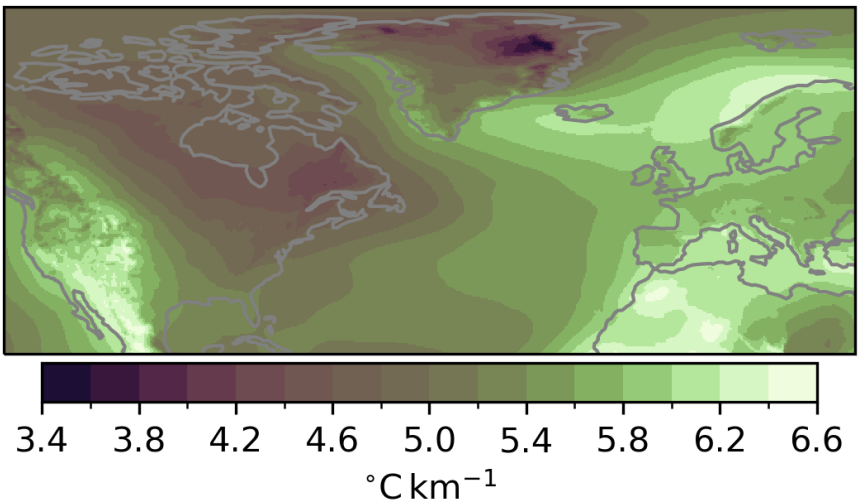

Figure S12. Climatological mean values of GAMMA during ONDJFM 1979–2022.

S4 Intensity measure evolution relative to genesis time

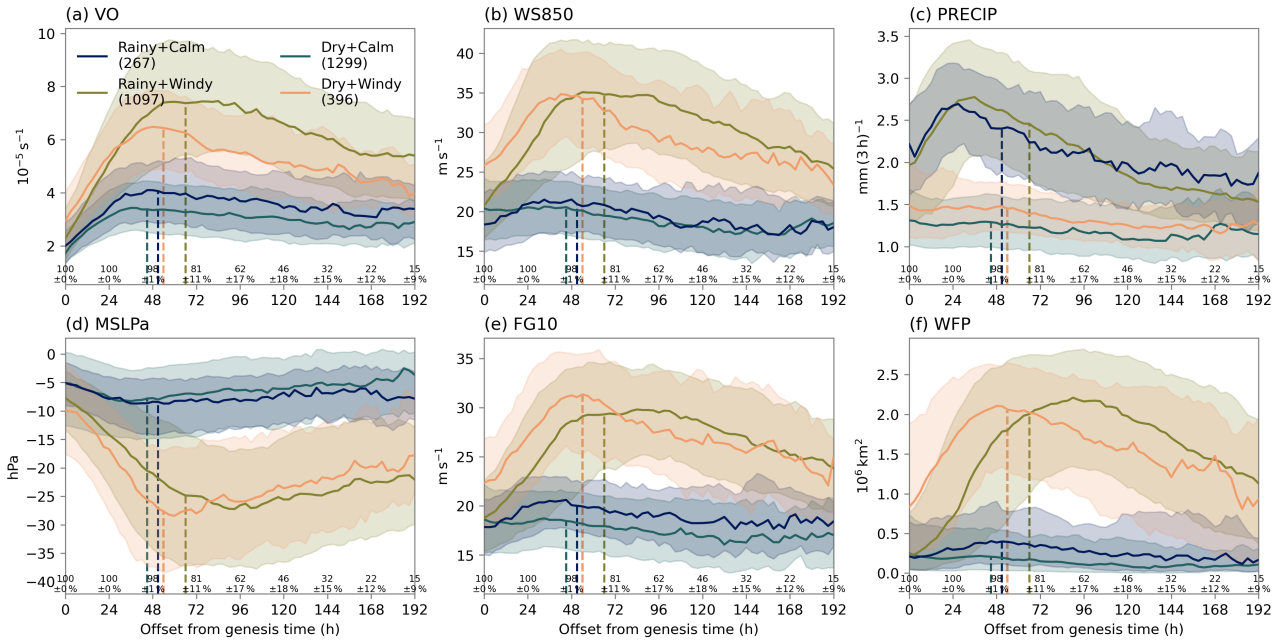

Figure S13. Evolution of six selected intensity measures in the four intensity groups relative to the time of genesis. The solid line shows the median value and the shading contains values in the two middle quartiles. Percentages on the x-axis show the mean and standard deviation of proportion of tracks sampled in the groups for a given time step. The complete group sizes are shown in parentheses in the legend in panel **(a)**. The dashed vertical lines indicate median times of maximum VO in the four groups.

References

Binder, H. and Wernli, H.: Frequency anomalies and characteristics of extratropical cyclones during extremely wet, dry, windy, and calm seasons in the extratropics, Wea. Climate Dyn., 6, 151–170, https://doi.org/10.5194/wcd-6-151-2025, 2025.

Cornér, J., Bouvier, C., Doiteau, B., Pantillon, F., and Sinclair, V. A.: Classification of North Atlantic and European extratropical cyclones using multiple measures of intensity, Nat. Hazards Earth Syst. Sci., 25, 207–229, https://doi.org/10.5194/nhess-25-207-2025, 2025.

Dacre, H. F. and Gray, S. L.: Quantifying the climatological relationship between extratropical cyclone intensity and atmospheric precursors, Geophys. Res. Lett., 40, 2322–2327, https://doi.org/10.1002/grl.50105, 2013.

Mbengue, C. O., Woollings, T., Dacre, H. F., and Hodges, K. I.: The roles of static stability and tropical–extratropical interactions in the summer interannual variability of the North Atlantic sector, Climate Dyn., 52, 1299–1315, https://doi.org/10.1007/s00382-018-4192-5, 2019.

Pfahl, S. and Sprenger, M.: On the relationship between extratropical cyclone precipitation and intensity, Geophys. Res. Lett., 43, 1752–1758, https://doi.org/10.1002/2016GL068018, 2016.